ELSEVIER

Journal of Alloys and Compounds 356–357 (2003) 773–778

Journal of ALLOYS AND COMPOUNDS

www.elsevier.com/locate/jallcom

Sn-containing (La,Mm)$Ni_{5-x}Sn_xH_{5-6}$ intermetallic hydrides: thermodynamic, structural and kinetic properties

O.Yu. Khyzhun[a], M.V. Lototsky[a], A.B. Riabov[a], C. Rosenkilde[b], V.A. Yartys[a,*], S. Jørgensen[c], R.V. Denys[d]

[a]*Institute for Energy Technology, P.O. Box 40, Kjeller, N-2027, Norway*
[b]*Norsk Hydro ASA, P.O. Box 2560, Porsgrunn, N-3901, Norway*
[c]*Center for Materials Research, University of Oslo, Oslo N-0349, Norway*
[d]*Physico-Mechanical Institute, National Academy of Sciences of Ukraine, 5, Naukova Str., Lviv, 79601, Ukraine*

Received 7 August 2002; received in revised form 15 January 2003; accepted 10 February 2003

Abstract

This work focused on studies of the phase composition and crystal structure of $La_xMm_{1-x}Ni_{4.7}Sn_{0.3}$ (x=0, 0.5 and 1.0) alloys, where Mm denotes La-rich mischmetal produced by Norsk Hydro ASA. The alloys have been studied using conventional powder and synchrotron X-ray diffraction (XRD), powder neutron diffraction and scanning electron microscopy (SEM). After annealing at 950 °C the alloys were nearly single-phase materials with small precipitations of RENiSn equiatomic intermetallics formed at grain boundaries. Hydrogen absorption–desorption studies at 298, 323 and 348 K showed (a) a 'flat' structure of the pressure–composition isotherms; (b) a rather broad range of working H storage capacities; (c) an increase of the plateau pressures and decrease in both enthalpy and entropy changes following an increase of the Mm content in the alloy; and (d) fast formation–decomposition rate. Desorption isotherms were approximated by a recently developed model of phase equilibria in the metal–hydrogen systems. In situ powder neutron diffraction studies of the system $MmNi_{4.7}Sn_{0.3}$–D_2 show that in the region of α-solid solution deuterium insertion leads to a gradual increase of the unit cell volume reaching 1.9%. In the hexagonal β-$MmNi_{4.7}Sn_{0.3}$ $D_{4.51}$ deuteride D atoms occupy two of four available types of tetrahedral interstices including 6*m* $RE_2(Ni,Sn)_2$ and 12*n* $RE(Ni,Sn)_3$.

Keywords: Metal hydrides; Intermetallics; Gas–solid reactions; Neutron diffraction; Thermodynamic modelling

1. Introduction

Hydrides of the $LaNi_5$-related alloys are widely used in different applications, including hydrogen storage and compression, H purification and separation, heat management and nickel–metal hydride batteries [1–3]. $LaNi_5$ has attractive hydrogen storage properties such as convenient desorption pressure slightly exceeding 1 bar at room temperature, extremely fast absorption and desorption kinetics and easy activation [3,4]. To achieve cost reduction, La in AB_5 alloys is replaced by Mischmetal (Mm), a natural mixture of the light rare earth metals, La, Ce, Pr and Nd. Chemical substitution of La by Mm and Ni by transition or nontransition elements significantly modifies the hydrogenation behaviour of $LaNi_5$ [3]. As example, the cycle stability of the hydrides is significantly improved by substitution of Ni with Al, Mn, Co and Sn [3]. Furthermore, corrosion resistance of AB_5 alloys is improved substantially due to the substitution of La with Mm [3]. Therefore, the Mm-based AB_5 alloys are of special interest for applications of MH.

Substitution of nickel by tin changes dramatically some properties of the parent $LaNi_5$ compound: the substitution leads to a significant decrease of the intrinsic degradation of the material [5] and to the increase of its cycling stability both with thermal cycling in hydrogen and in an electrochemical cell [6–8]. $LaNi_{4.75}Sn_{0.25}$ shows the best hydrogen storage capacity and cycling lifetime for as-cast and annealed $LaNi_{5-x}Sn_x$ alloys [7].

Hydrides of the Sn-substituted $LaNi_{5-x}Sn_x$ (x=0–0.5) were studied in Refs. [8–11]. It was found that a small substitution of nickel by tin decreases substantially the plateau pressure, however, the plateau width decreases

*Corresponding author. Tel.: +47-63-806-453; fax: +47-63-810-920.
E-mail address: volodymyr.yartys@ife.no (V.A. Yartys).

0925-8388/03/$ – see front matter
doi:10.1016/S0925-8388(03)00352-9

insignificantly with increasing x [8,11]. Increase of enthalpies of formation of the $LaNi_{5-x}Sn_xH_y$ is proportional to x, while the plateau entropy is nearly independent of x.

This work was focused on studies of phase composition, crystal structure and H sorption properties of Mm-substituted AB_5 alloys $La_xMm_{1-x}Ni_{4.7}Sn_{0.3}$.

2. Experimental

Norsk Hydro ASA used rare earth chlorides to electrolytically produce the La-rich mischmetal used in this work. Composition of the Mm was analysed by Induction Coupled Plasma exited absorption spectroscopy and a Glow Discharge Mass Spectrometry (GDMS) method. Analysis showed that the Mm contained 58.0 wt.% La, 28.6 wt.% Ce, 5.8 wt.% Pr and 7.5 wt.% Nd. The GDMS data indicated also a presence of some impurities, with Al (360 ppm) and S (350 ppm) being the highest. Purity of La, Ni and Sn, was higher than 99.9 at.%. Intermetallic alloys with composition $La_xMm_{1-x}Ni_{4.7}Sn_{0.3}$, where $x=$ 0.0, 0.5 and 1.0, were prepared by argon arc-melting of stoichiometric mixtures of the components. Then, ~5 g ingots were annealed in vacuum for 1 month at 500 °C and water-quenched after annealing. The samples were in addition annealed at 950 °C for 1 week, with a subsequent quenching into an ice–water mixture.

A powder X-ray diffraction (PXD) study was performed using a Siemens D5000 diffractometer with $CuK\alpha_1$ radiation (Bragg Brentano geometry, position sensitive detector). Synchrotron radiation (SR) PXD data were collected with the powder diffracrometer (in Debye-Scherrer mode) at the Swiss-Norwegian Beam Line (BM1) at ESRF (Grenoble, France). Monochromatic X-rays ($\lambda=0.49868$ Å) were obtained from a Si(111) crystal. The samples were kept in a rotating 0.3-mm diameter sealed glass capillary.

Scanning electron microscopy (SEM) was used for the characterisation of microstructures and for the microprobe element analysis. The SEM data were derived using a Philips XL 30 microscope equipped with energy dispersive X-ray analysis (EDS). The sample surfaces were polished with different diamond pastes and were covered with a thin layer of gold before the SEM experiment.

The PND data for $MmNi_{4.7}Sn_{0.3}$-based deuteride were measured in situ in deuterium gas with the D1B instrument ($\lambda=2.525$ Å), ILL. The sample was kept in a quartz container allowing to reach deuterium pressures up to 4 bar. Deuterium loading started at 318 K and $P=2$ bar D_2 with a formation of a solid solution of deuterium in the intermetallic lattice. After decreasing the temperature to 313 K and increasing deuterium pressure to >3 bar, the β-deuteride started to form. The temperature was kept constant at $T=313$ K until the sample was saturated with deuterium. The D1B diffractometer is equipped with a multidetector (400 cells) covering an angular 2θ range of 80° with a step of 0.2.

The refinements of the data were performed using the General Structure Analysis Software and the following neutron scattering lengths taken from the GSAS library: $b_{La}=8.24$; $b_{Ce}=4.84$; $b_{Pr}=4.58$; $b_{Nd}=7.69$; $b_{Ni}=10.20$; $b_{Sn}=6.23$; $b_D=6.67$ fm. The hydrogen sorption/desorption characteristics were measured volumetrically (Sievert's method) in the pressure range 0.001–25 bar H_2 using a hydrogenation apparatus designed at the Laboratoire de Chimie Metallurgique des Terres Rares (CNRS, Thiais-Paris, France) and described in [11]. The samples were hydrogenated and decomposed four to five times before measuring their desorption isotherms.

The sets of experimental desorption isotherms for each alloy were approximated by the model for the simulation of PCT diagrams, proposed in Ref. [12].

3. Results and discussion

PXD and SR PXD studies indicate that all studied $La_xMm_{1-x}Ni_{4.7}Sn_{0.3}$ samples after annealing at 500 °C were two-phase, containing tin-rich ($La_xMm_{1-x}Ni_{\sim4.5}Sn_{\sim0.5}$) and tin-poor ($La_xMm_{1-x}Ni_{\sim4.9}Sn_{\sim0.1}$) AB_5 intermetallics. As an example, Fig. 1 shows the PXD pattern obtained for $LaNi_{4.7}Sn_{0.3}$. The sample contains a mixture of two phases, $LaNi_{\sim4.9}Sn_{\sim0.1}$ with unit cell parameters $a=$ 5.036(3) Å and $c=3.994(3)$ Å (major constituent) and $LaNi_{\sim4.5}Sn_{\sim0.5}$ with unit cell parameters $a\sim5.10$ Å and $c\sim4.07$ Å (minor constituent).

After further annealing at 950 °C for 1 week, all three samples became single-phase materials, as shown by the refinements of the SR PXD data (see Fig. 2 as example). Earlier, during a single crystal XRD study of similar alloys, $LaNi_{4.7}Sn_{0.3}$, $LaNi_{4.6}Sn_{0.4}$ and $LaNi_{4.5}Sn_{0.5}$ [11], it has been found that Sn has a significant preference in the occupation of the 3g position which is more distanced from La. In the chemically related $LaNiSnD_2$ [13] and NdNiSnD [14], a mutual substitution of Ni and Sn (10%) takes place. Such solubility seems to be typical for the systems containing rare earth metals, Ni and Sn. The detailed results concerning a distribution of Sn in the crystal lattice of the studied alloys will be published elsewhere.

The lattice parameters of the samples annealed at 950 °C samples are listed in Table 1. Data for $LaNi_{4.7}Sn_{0.3}$ are in good agreement with the reference data [15]. As can be seen from Table 1, both a parameter and the unit cell volume V of $La_{1-x}Mm_xNi_{4.7}Sn_{0.3}$ decrease with increasing x, while the c parameter and c/a show a trend of rising following an introduction of Mm into the composition of the alloy, on a transition from $LaNi_{4.7}Sn_{0.3}$ to $La_{0.5}Mm_{0.5}Ni_{4.7}Sn_{0.3}$ and $MmNi_{4.7}Sn_{0.3}$. From reference

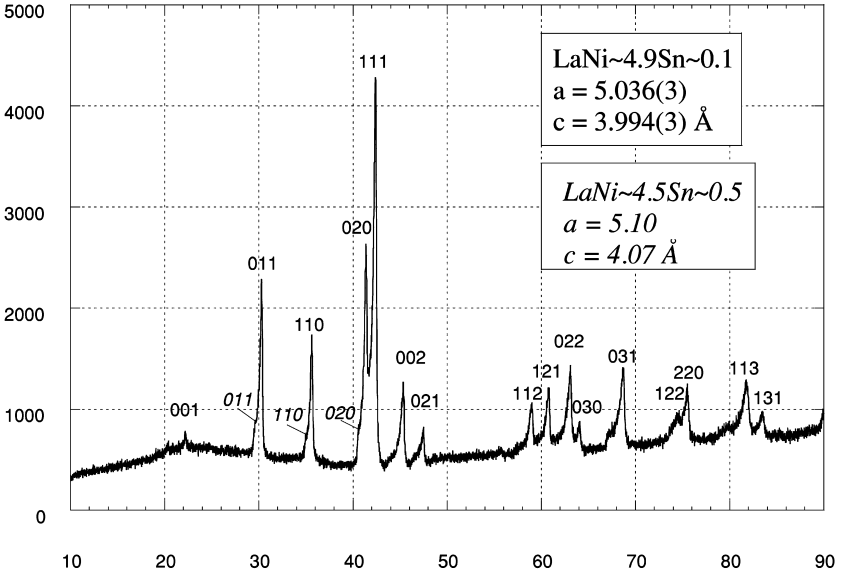

Fig. 1. PXD pattern of $LaNi_{4.7}Sn_{0.3}$ annealed at 500 °C for 1 month (Cu $K\alpha_1$ radiation).

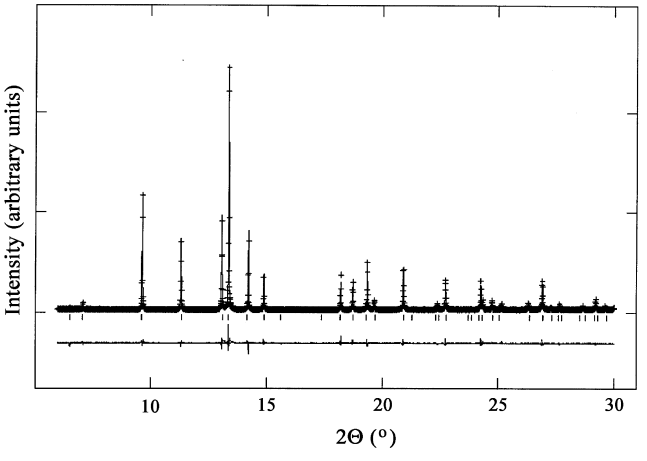

Fig. 2. SR PXD pattern of $LaNi_{4.7}Sn_{0.3}$ annealed at 950 °C for 1 week showing observed (+), calculated (—) and difference (___) plots. λ = 0.49868 Å. The positions of the peaks are marked.

data [16], a transition from La- to the Ce-containing RNi_5 intermetallic is accompanied by similar modifications of the crystallographic parameters (see Table 1) as were observed in the present work. Thus, these changes are related to a substitution of La in the AB_5 alloy by Ce, the second main constituent of the Mischmetal used.

Table 1
Lattice parameters and unit cell volumes of the studied compounds

Alloy	a (Å)	c (Å)	c/a	V (Å^3)
$LaNi_5$ [16]	5.017	3.987	0.795	86.91
$LaNi_{4.7}Sn_{0.3}$	5.06077(4)	4.02970(4)	0.796	89.38(2)
$La_{0.5}Mm_{0.5}Ni_{4.7}Sn_{0.3}$	5.0415(1)	4.0486(1)	0.803	89.113(5)
$MmNi_{4.7}Sn_{0.3}$	5.0282(1)	4.04814(8)	0.805	88.636(4)
$CeNi_5$ [16]	4.874	4.004	0.821	82.37

The data from the SEM studies shown in Fig. 3 are in agreement with the results of the PXD and SR PXD investigations: all alloys studied are nearly single phase materials with small amount of impurity (<1 vol.%) of RENiSn equiatomic intermetallics ($LaNi_{4.7}Sn_{0.3}$ and $La_{0.5}Mm_{0.5}Ni_{4.7}Sn_{0.3}$) and $MmNi_{4.5}Sn_{0.5}$ compound ($MmNi_{4.7}Sn_{0.3}$). Impurities concentrate along the grain boundaries of the major phase (Fig. 3c). As can be seen from Fig. 3, the studied samples are very porous materials containing cracks. The grains are rather large and have a columnar shape.

All studied samples absorb hydrogen very quickly, and reach the saturation values of $H/La_xMm_{1-x}Ni_{4.7}Sn_{0.3} \approx$ 5.5–5.9 ($H/M \approx 0.92$–0.98) within 1 to 2 min. Beginning from the second hydrogenation/desorption cycle, hydrogen absorption and desorption isotherms became completely reproducible.

An in situ powder neutron diffraction study of deuterium absorption by $MmNi_{4.7}Sn_{0.3}$ showed three stages of interaction of the alloy with D_2 including (a) formation of α-solid solution (stage I); (b) nucleation and growth of the β-phase in the two-phase region α+β (Stage II); (c) saturation of the β-phase by deuterium within the homogeneity region of the β-phase (Stage III). In the present paper we will focus on stages I and II. It is interesting that within the range of the α-solid solution, an increase of overall D content is associated with a gradual linear increase of the unit cell volume reaching finally 1.9% ($\Delta a/a = 0.7\%$, $\Delta c/c = 0.5\%$) at the end of stage I (Fig. 4). Deuterium atoms in the α-phase enter predominantly the 6*m* sites.

Formation of the β-deuteride (space group $P6/mmm$; $a = 5.3208(7)$; $c = 4.2448(7)$ Å; $V = 104.07$ Å^3) is accompanied by a volume expansion of ~17.4%. A four-site model ($6m + 12n + 12o + 4h$) of the deuterium sublattice

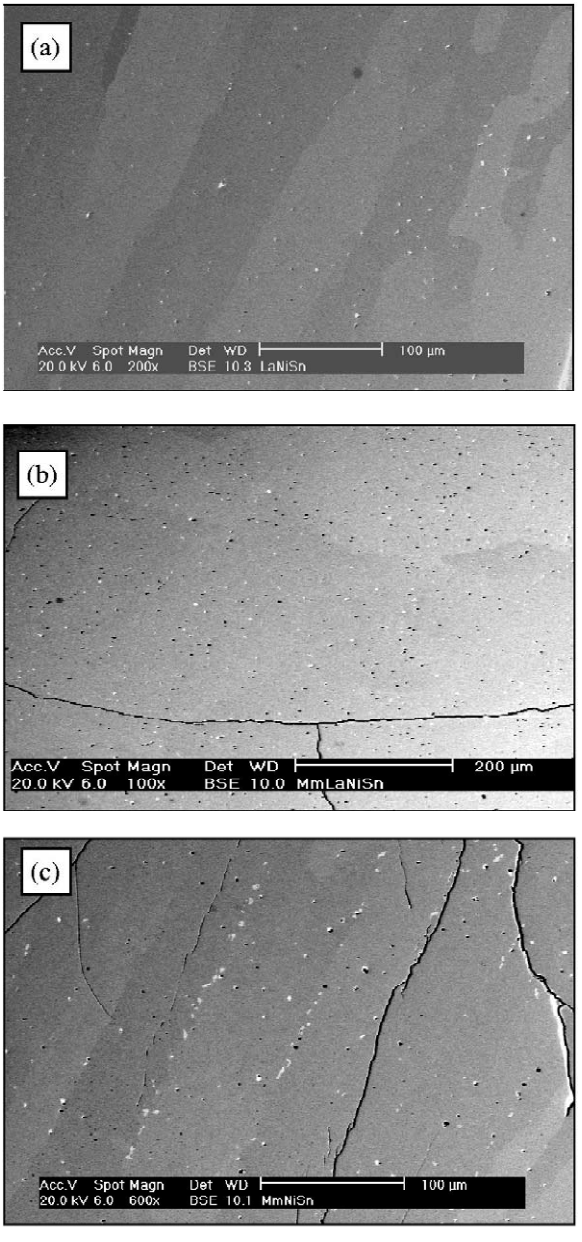

Fig. 3. Back scattered SEM images of $LaNi_{4.7}Sn_{0.3}$ (a), $La_{0.5}Mm_{0.5}Ni_{4.7}Sn_{0.3}$ (b) and $MmNi_{4.7}Sn_{0.3}$ (c).

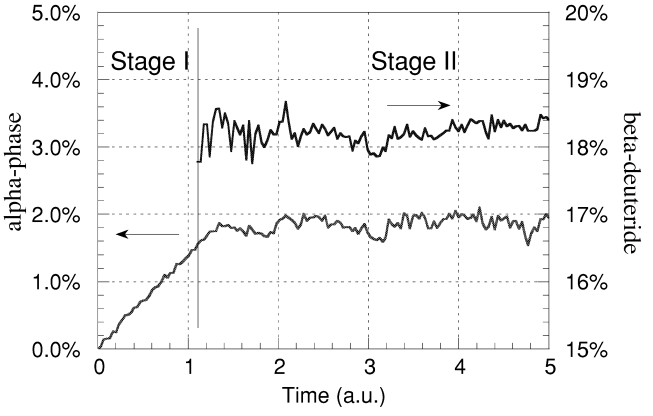

Fig. 4. Evolution of the increments of the unit cell volumes, $\Delta V/V$, for the α-phase and β-deuteride during deuterium absorption by $MmNi_{4.7}Sn_{0.3}$ from the analysis of the PND data.

was employed in the Rietveld profile refinements. The refinements yielded a stoichiometric composition D/$MmNi_{4.7}Sn_{0.3}$ = 4.51 resulting from the occupancy of the 6*m* $Mm_2(Ni,Sn)_2$ (30.9%) and 12*n* $Mm(Ni,Sn)_3$ (22.1%) sites. The observed occupation numbers are close to those reported for the 6*m* and 12*n* sites in the structures of $LaNi_{4.5-4.8}Sn_{0.2-0.5}$ $D_{5.2-6.1}$ [11]. However, in contrast with the reference data [11], two other sites (12*o* and 4*h*) are completely vacant. Possible reason for such a difference is a smaller D content in the studied deuteride compared to the reference data where it exceeded 5.2 at.D/f.u. A decrease of D content leads to an early removal from the sites with the smallest binding energy and the lowest occupation numbers, 12*o* and 4*h*. There is a clear correlation between the size of the volume effects on deuteration and D content in the deuterides observed in the present work and reported in [11]. Indeed, both V and $\Delta V/V$ are smaller in comparison with similar $LaNi_{4.5-4.8}Sn_{0.2-0.5}$-based deuterides reported in [11] (108.6–108.7 $Å^3$ and 18.5–22.2%), in agreement with a lower D content in $MmNi_{4.7}Sn_{0.3}D_{4.51}$.

Furthermore, the D content in the studied deuteride is smaller than the overall hydrogen storage capacity of $La_xMm_{1-x}Ni_{4.7}Sn_{0.3}H_x$ obtained from the volumetric PCT measurements (end of desorption plateau) of approximately 5.5 at.H/f.u. Smaller deuterium content in the sample studied by NPD is caused by

(a) Absorption pressures applied in the in situ measurements were limited to 4 bar D_2;
(b) Type of experiments: absorption instead of desorption;
(c) Smaller amount of cycles applied to activate the alloy in case of deuteride (2) compared to the PCT measurements on the corresponding hydrides (>5).
(d) Possible isotope effects.

Hydrogen absorption–desorption studies at 298, 323 and 348 K showed (a) a 'flat' structure of the pressure–composition isotherms; (b) a rather broad range of working H storage capacities; (c) an increase of the plateau pressures and decrease in both enthalpy and entropy changes following an increase of the Mm content in the alloy; and (d) fast formation–decomposition rate.

Hydrogen desorption isotherms presented in Fig. 5, are shown as sets of experimental points and calculated curves obtained by fitting of the latter using the model reported in [12]. This model is able to quantitatively describe phase equilibria in the metal–hydrogen systems. It is based on a consideration of both attractive and repulsive interactions between interstitial hydrogen dissolved in the metal matrix.

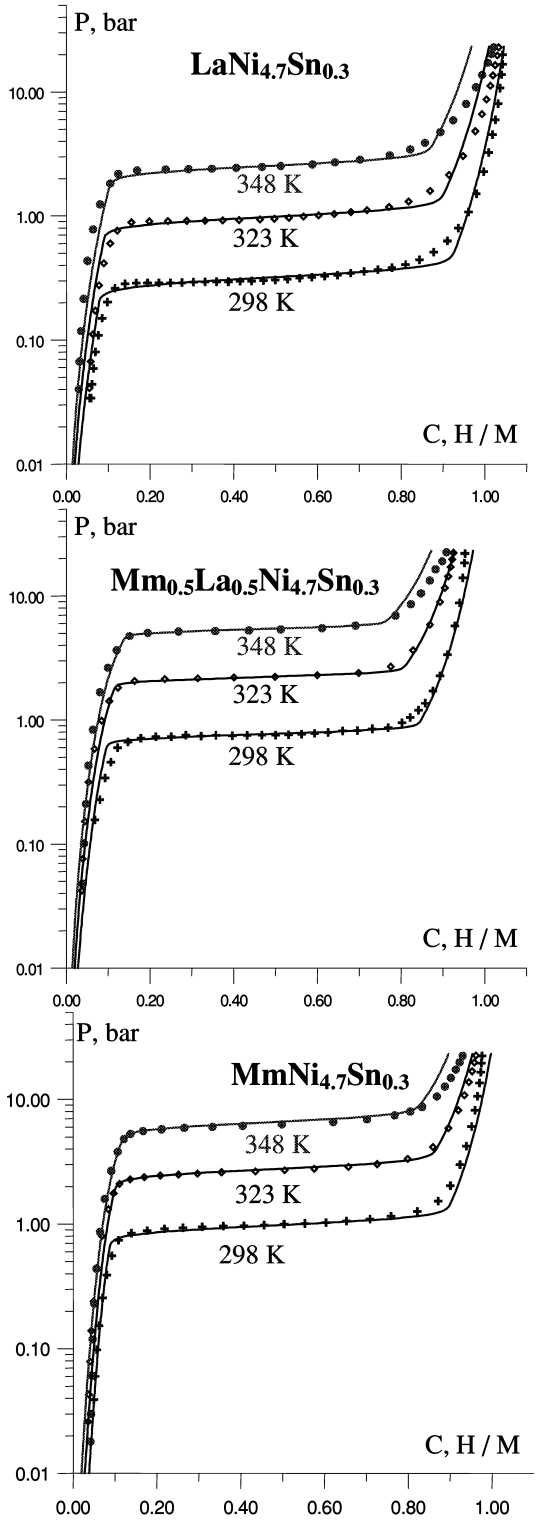

Fig. 5. Hydrogen desorption isotherms in the systems (La,Mm)$Ni_{4.7}Sn_{0.3}$–H_2: experimental points and calculated curves.

The model describes the asymmetry of the experimental 'pressure–composition' isotherms, temperature-dependent plateau slopes and smooth transitions between α-, (α+β)- and β-regions. It postulates an existence of local fluctuations in the stoichiometric composition of the alloys causing an appearance of statistical deviations of the correlated values of entropy and enthalpy from their corresponding mean values.

From Table 2 and Fig. 5 it is evident that a substitution of La by Mm causes a decrease of the stability of the hydride and slightly decreases H sorption capacity of the alloys.

One problem in fitting was an existence of residual hydrogen concentration $C_{min}>0$ observed at $P\rightarrow 0$. It is similar to the behaviour of $TiCr_{\sim 2}$–H system [17]. The corresponding correction was made by introducing an imaginary 'zero' plateau segment having the fraction g_0 which value, according to the calculations (Table 2), is in the range from 6 to 10%.

All experimental data sets were approximated with essentially the same accuracy corresponding to $(2\ldots 3)\cdot 10^{-2}$ H/M. Comparison of experimentally measured and calculated H sorption capacities at $P=20$ bar, as well as standard enthalpies and entropies of hydrogenation at H/M=0.5 (Table 3) also shows a good agreement for all alloys. The enthalpies show a trend of decreasing of the thermal stability of the $Mm_{1-x}La_xNi_{4.7}Sn_{0.3}$-based hydrides following a replacement of lanthanum by mischmetal. According to the calculations, the replacement lowers the critical temperatures, T_c. In addition, the replacement of La with Mm also results in increasing the non-ideal shape of the isotherms (plateau slope and fuzziness of limits of plateau region) which is reflected by an increase of the deviations in σ_S and σ_H.

The observed values $\Delta H^o=-36.5\pm 0.1$ kJ/(mole H_2) and $\Delta S^o=-112.6\pm 0.1$ J/(K mole H_2) for $LaNi_{4.7}Sn_{0.3}$ (Table 3) are in good agreement with the values $\Delta H^o=-37.0$ kJ/(mole H_2) and $\Delta S^o=-109.2$ J/(K mole H_2) derived in [8] for the similar compound $LaNi_{4.68}Sn_{0.32}$.

In conclusion, the substitution of La with Mm produced by Norsk Hydro ASA results in increase of the plateau pressure, remaining however below 1 bar at room temperature for all the samples. It indicates that the usage of the commercial La-rich Mm to produce H storage alloys belonging to the AB_5 family is very prospective. Their very good absorption–desorption characteristics can be successfully utilised in a number of technological applications adjusted to the most convenient 'ambient' P–T conditions.

Acknowledgements

This work has received a support from the Norwegian Research Council and from Norsk Hydro ASA. We are indebted to the Institut Laue Langevin of Grenoble, France for the provision of neutron facilities. The skilful assistance from the project team at the Swiss–Norwegian Beam Line, ESRF, Grenoble, is gratefully acknowledged.

We are grateful to A. Percheron-Guégan, M. Latroche,

Table 2
PCT fitting parameters for the systems $Mm_{1-x}La_xNi_{4.7}Sn_{0.3}$–$H_2$ ($x=0$; 0.5; 1.0)

Parameter	$LaNi_{4.7}Sn_{0.3}$	$Mm_{0.5}La_{0.5}Ni_{4.7}Sn_{0.3}$	$MmNi_{4.7}Sn_{0.3}$
Maximum H concentration, C_{max} (H/M)	1.26	1.21	1.24
'Zero' segment fraction, g_0	0.10	0.10	0.06
Critical temperature, T_c (K)	483.0	426.8	416.3
Entropy contribution into concentration-independent term of $P(C,T)$, ΔS_o (J/(mole·K))	−102.1	−105.3	−102.5
Enthalpy contribution into concentration-independent term of $P(C,T)$, ΔH_o (kJ/mole)	−13.0	−14.5	−13.5
Entropy deviation, σ_S (J/(mole·K))	0.09	0.69	1.50
Enthalpy deviation, σ_H (kJ/mole)	0.38	0.37	0.51
Correlation coefficient, ρ_{SH}	0.977	0.962	0.857
Estimated error in H/M	0.03	0.02	0.02

Table 3
Calculated and experimental H sorption capacities and standard enthalpies and entropies of hydrogenation

Starting IMC	T (K)	H/M (H/AB_5) at $P=20$ bar		ΔH° (kJ/mole)		ΔS° (J/(mole·K))	
		Experimental	Calculated	Experimental	Calculated	Experimental	Calculated
$LaNi_{4.7}Sn_{0.3}$	298	1.04 (6.24)	1.04 (6.24)	−36.51	−36.85	−112.6	−111.2
	323	1.03 (6.18)	1.01 (6.06)				
	348	1.02 (6.12)	0.96 (5.76)				
$Mm_{0.5}La_{0.5}Ni_{4.7}Sn_{0.3}$	298	0.95 (5.70)	0.97 (5.82)	−33.80	−33.62	−111.2	−109.6
	323	0.92 (5.52)	0.92 (5.52)				
	348	0.90 (5.40)	0.86 (5.16)				
$MmNi_{4.7}Sn_{0.3}$	298	0.97 (5.82)	1.00 (6.00)	−31.83	−32.16	−106.8	−106.8
	323	0.96 (5.76)	0.95 (5.70)				
	348	0.92 (5.52)	0.89 (5.34)				

J.M. Joubert (CNRS, Thiais, France) for the generous help in the provision of the PCT equipment. We thank O. Isnard (CNRS, Grenoble, France) and B.C. Hauback (IFE) for the cooperation in the PND and SR XRD measurements.

References

[1] P. Dantzer, Hydrogen in metals III. Properties and Applications, in: H. Wipf (Ed.), Topics in Applied Physics, Vol. 73, Springer-Verlag, Berlin, 1997, p. 279.
[2] T. Sakai, H. Yoshinaga, H. Miyamura, N. Kuriyama, H. Ishikawa, J. Alloys Comp. 180 (1992) 37.
[3] T. Sakai, M. Matsuoka, C. Iwakura, in: K.A. Gschneider Jr., L. Eyring (Eds.), Handbook on the Physics and Chemistry of Rare Earths, Vol. 21, Elsevier, Amsterdam, 1995, p. 133, Chapter 142.
[4] J.S. Cantrell, T.A. Beiter, R.C. Bowman Jr., J. Alloys Comp. 207/208 (1994) 372.
[5] S.W. Lambert, D. Chandra, W.N. Cathey, F.E. Lynch, R.C. Bowman Jr., J. Alloys Comp. 187 (1992) 113.
[6] R.C. Bowman Jr., C.H. Luo, C.C. Ahn, C.K. Witham, B. Fultz, J. Alloys Comp. 217 (1995) 185.
[7] B.V. Ratnakumar, C. Witham, R.C. Bowman Jr., A. Hightower, B. Fultz, J. Electrochem. Soc. 143 (1996) 2578.
[8] S. Luo, W. Luo, J.D. Clewley, T.B. Flanagan, L.A. Wade, J. Alloys Comp. 231 (1995) 467.
[9] M. Mendelsohn, D. Gruen, A. Dwight, Mater. Res. Bull. 13 (1978) 1221.
[10] F. Oliver, W. Morgan, E. Hammond, S. Wood, L. May, J. Appl. Phys. 57 (1985) 3250.
[11] J.-M. Joubert, M. Latroche, R. Černý, R.C. Bowman Jr., A. Percheron-Guégan, K. Yvon, J. Alloys Comp. 293–295 (1999) 124.
[12] M.V. Lototsky, V.A. Yartys, V.S. Marinin, N.M. Lototsky, J. Alloys Comp. (2003) in press.
[13] V.A. Yartys, T. Olavesen, B.C. Hauback, H. Fjellvåg, H.W. Brinks, J. Alloys Comp. 330–332 (2002) 141.
[14] V.A. Yartys, T. Olavesen, B.C. Hauback, H. Fjellvåg, J. Alloys Comp. 336 (1–2) (2002) 181.
[15] T. Vogt, J.J. Reilly, J.R. Johnson, G.D. Adzic, J. McBreen, Electrochem. Solid State Lett. 2 (3) (1999) 111.
[16] E.I. Gladyshevskyi, O.I. Bodak, Crystal chemistry of intermetallic compounds of the rare earth metals, Lviv. Vyszcza Shkola, 1982.
[17] O. Beeri, D. Cohen, Z. Gavra, J.R. Johnson, M.H. Mintz, J. Alloys Comp. 267 (1998) 113.